Journal of Applied Pharmaceutical Research
Volume 13 Issue 2, Year of Publication 2025, Page 181 – 193
DOI: https://doi.org/10.69857/joapr.v13i2.1037

Check for updates

Research Article

JOURNAL OF APPLIED PHARMACEUTICAL RESEARCH | JOAPR
www.japtronline.com ***ISSN: 2348 – 0335***

FORMULATION AND OPTIMIZATION OF UPADACITINIB-LOADED TRANSDERMAL PATCHES FOR RHEUMATOID ARTHRITIS WITH ZERO-ORDER RELEASE KINETICS

Shubham Talole, Rahul Godge*, Nikita Tambe, Nikita Mhase

Article Information
Received: 24th January 2025
Revised: 18th March 2025
Accepted: 12th April 2025
Published: 30th April 2025

Keywords
Upadacitinib, Transdermal patch, Factorial design, Zero-order kinetics, PVP K30, HPMC K4M, JAK inhibitor

ABSTRACT
Background: To develop and optimize Upadacitinib-loaded transdermal patches for rheumatoid arthritis treatment with improved patient compliance and sustained drug delivery. **Methodology:** Upadacitinib transdermal patches were formulated using a 3^2 factorial design approach with PVP K30 and HPMC K4M as key polymeric components. The patches were characterized for physicochemical, mechanical, and ex vivo permeation properties. **Results and Discussion:** The optimized formulation (SF8) exhibited excellent physicochemical characteristics, including high drug content (99.05 ± 0.83%), optimal mechanical properties with tensile strength of 0.912 kg/mm² and adhesion strength of 3.94 N. The ex vivo permeation reached 86.35% at 12h, with the flux of 102.91 µg/cm²/h following zero-order kinetics (R^2 = 0.9777). The experimental values closely matched predicted values with less than 2% error. Accelerated stability studies confirmed minimal changes in critical parameters over six months. **Conclusion:** The optimized Upadacitinib transdermal patch provides sustained drug delivery with zero-order release kinetics and excellent stability. This transdermal delivery system offers a promising alternative to oral therapy with potential advantages of improved patient compliance, reduced dosing frequency, and avoidance of first-pass metabolism for rheumatoid arthritis management.

INTRODUCTION

Rheumatoid arthritis (RA) constitutes a major global public health priority, in which an estimated 14 million individuals suffer from RA in a population prevalence of 0.24%. This is a chronic autoimmune disorder with significant economic and healthcare burdens, which resulted in direct medical costs exceeding $19 billion per year in the United States alone and $39 billion in indirect costs associated with work disability and decreased productivity [1]. Currently, the management of RA is based on conventional disease-modifying antirheumatic drugs (DMARDs), biological agents, and small-molecule inhibitors, which are administered orally or parenterally. Nevertheless, these methods of delivery are limited in various ways, including systemic adverse effects, inconsistent drug plasma concentration, complicated patient compliance, and prohibitively high cost of treatment. Given that therapeutic advances have only reduced the likelihood of inadequate disease control to approximately 40% in recent epidemiological data, innovative drug delivery systems are needed to provide more effective therapy with less adverse effects [2].

*Department of Pharmaceutical Quality Assurance, Pravara Rural College of Pharmacy, Pravaranagar
***For Correspondence:** **rahulgodge@gmail.com**

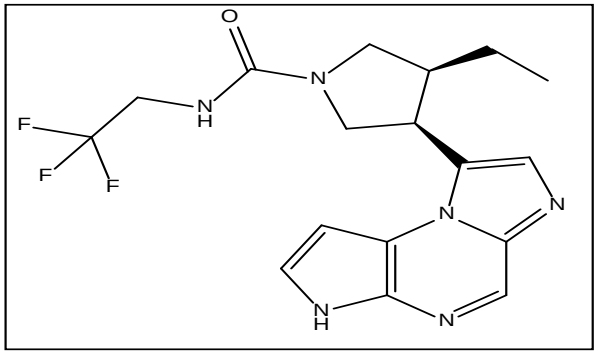

Figure 1: Chemical Structure of Upadacitinib

Selective Janus kinase 1 (JAK1) inhibitor upadacitinib has been identified as a promising agent for the management of RA. With a molecular weight of 389.38 g/mol, this small molecule is highly selective for JAK1 over JAK2, JAK3, and TYK2 and makes it well suited for favorable efficacy-safety profile. Upadacitinib retains a cyanoacetyl group that is key to its potency and selectivity. Physicochemical properties of the compound in terms of optimal lipophilicity (log P: 2.3) adequate aqueous solubility (14 mg/mL at pH 7.4) and molecular size are excellent with regard to transdermal delivery [3]. Upadacitinib mechanism of action is to directly inhibit JAK1-mediated STAT phosphorylation down-regulating the expression of proinflammatory cytokines linked to RA pathophysiologic mechanism. Results from clinical studies show that upadacitinib significantly improves ACR20 response rates (71% vs. 36%, $p< 0.001$) compared with placebo as well as better efficacy than adalimumab on reducing disease activity score in 28 joints (DAS28) [4].

RA management is particularly suitable with transdermal drug delivery systems (TDDS) which provide several benefits. These systems sustain and control drug release, avoid hepatic first pass metabolism and have controlled drug delivery with reduced dosing frequency. Development of various permeation enhancers, microneedle arrays, nanocarrier based systems have enabled the contemporary transdermal technology to overcome the stratum corneum barrier and enhance drug penetration [5]. As matrix type transdermal patches incorporating permeation enhancers, such as oleic acid and propylene glycol, are capable of dissolving the intercellular lipid in the stratum corneum and facilitate the delivery of the payload for upadacitinib, these are a promising approach for the delivery of upadacitinib. Further advances in pressure sensitive adhesives (PSA) have increased patch adhesion properties and drug loading capacity. Furthermore, TDDS are in line with the increasing focus on patient centred care and provide non-invasive, self-administered treatment options that might increase adherence and overall quality of life in RA patients [6].

The current Rheumatoid Arthritis (RA) treatment framework produces three main issues due to medication adverse effects on patient compliance and inconsistent plasma drug amounts alongside frequent dosage requirements [7]. A transdermal delivery system of Upadacitinib resolves current gaps through long-term systemic drug release alongside hepatic first-pass avoidance and fewer required doses which can increase patient adherence [8]. The delivery method proves essential for RA patients who face challenges because of their joint pain along with mobility restrictions when they need to take daily oral medicine. Transdermal delivery systems offer steady drug plasma levels compared to oral formulations thus they lead to better therapy results besides diminishing systemic adverse effects [9].

The objective of the present study is to formulate and optimize a Upadacitinib loaded transdermal patch for better management of rheumatoid arthritis. Specifically, the objectives are developing a stable matrix type transdermal patch with optimized drug loading and release kinetics, evaluating the effect of different permeation enhancers on transdermal delivery of upadacitinib, studying physical and chemical characterization (*in vitro* release profile, *ex vivo* permeation), patch stability in accelerated condition and the effects of the method on particle properties.

MATERIALS AND METHODS

Materials

Upadacitinib (pharmaceutical grade, ≥99.5% purity) was obtained as a gift sample from supplier Sciquaint Innovation (Pune, India). Polyvinylpyrrolidone K30 (PVP K30) (pharmaceutical grade, MW 40,000 Da) and Hydroxypropyl methylcellulose K4M (HPMC K4M) (pharmaceutical grade) was procured from Sciquaint Chemicals. (Pune, India). Propylene glycol (analytical grade, 99.5% purity) and Oleic acid (analytical grade, ≥99.0% purity) was obtained from Neeta chemicals (Pune, India). Ethanol (HPLC grade, 99.9% purity) and Backing membrane (polyethylene film, 0.1 mm thickness) and Methanol (HPLC grade, ≥99.9% purity) was purchased from Research Lab fine chem industries (Mumbai, India). All other chemicals and reagents used in the study were of analytical grade and used as received without further purification.

Methods

FTIR Analysis

Potential drug-polymer interaction was evaluated by Fourier Transform Infrared (FTIR) spectroscopy. Pure Upadacitinib, physical mixtures of the drug with polymers, and optimized transdermal patch formulation were analyzed by an FTIR spectrophotometer equipped with an ATR accessory (Shimadzu India, IR Affinity-1S) from 3600 to 400 cm^{-1}. Finally, samples were dropped directly onto a diamond crystal and scanned in the wavenumber range of 4000–400 cm^{-1} with a resolution of 4 cm^{-1} using 32 scans per spectrum. Before every sample analysis, background measurements were taken. LabSolutions IR software (version 2.21, Shimadzu, India) was used to analyze the FTIR spectra and discover the characteristic peaks and possible interactions [10]. All the measurements were performed in triplicate (n=3) at room temperature (25±2°C) [11].

Experimental Design

A 3^2 full factorial design was implemented to optimize the Upadacitinib-loaded transdermal patch formulation. Two independent variables were selected: concentration of polyvinylpyrrolidone (PVP K30) (X_1) and concentration of hydroxypropyl methylcellulose (HPMC K4M) (X_2), each at three levels (low, medium, and high). The dependent variables were ex vivo drug permeation at 12 hours (Y_1) and patch adhesion strength (Y_2). Design-Expert software (version 12.0, Stat-Ease Inc., Minneapolis, USA) was used for experimental design generation, analysis, and optimization. The polynomial equation used to analyze the experimental outcomes was:

$$Y = b_0 + b_1X_1 + b_2X_2 + b_{12}X_1X_2 + b_{11}X_1^2 + b_{22}X_2^2$$

Where Y represents the dependent variable, b_0 is the arithmetic mean response of all experimental runs, b_1 and b_2 are the coefficients of the main effects, b_{12} is the coefficient of the interaction effect, and b_{11} and b_{22} are the coefficients of the quadratic terms. Statistical significance was determined at $p < 0.05$ [12]. While the 3^2 factorial design effectively optimized the Upadacitinib transdermal patch formulation, specific limitations should be noted. The selected polymer concentration ranges may not capture effects at ratios outside these boundaries, and the design maintained constant permeation enhancer concentration, plasticizer content, and solvent volume, potentially overlooking their influence. Additionally, the approach did not account for molecular-level polymer-drug interactions during storage or skin condition variations in rheumatoid arthritis patients that might affect clinical performance. Nevertheless, the design successfully identified the optimal polymer combination balancing adhesion strength and drug permeation for this therapeutic application.

Table 1: Variables in 3^2 Factorial Design for Upadacitinib Transdermal Patch

Independent Variables	Levels (mg)		
	Low (-1)	Medium (0)	High (+1)
X_1: PVP K30	40	70	100
X_2: HPMC K4M	20	40	60
Dependent Variables			**Goal**
Y_1: Ex vivo Drug permeation at 12h (%)			Maximize
Y_2: Adhesion strength (N)			Maximize

Table 2: Composition of Upadacitinib Transdermal Patch Formulations

Ingredients	SF1	SF2	SF3	SF4	SF5	SF6	SF7	SF8	SF9
Upadacitinib (mg)	15	15	15	15	15	15	15	15	15
PVP K30 (mg)	40	40	40	70	70	70	100	100	100
HPMC K4M (mg)	20	40	60	20	40	60	20	40	60
Propylene glycol (mL)	0.2	0.2	0.2	0.2	0.2	0.2	0.2	0.2	0.2
Oleic acid (mg)	10	10	10	10	10	10	10	10	10
Ethanol(mL)	8	8	8	8	8	8	8	8	8

Preparation of Transdermal Patch

Transdermal patches were prepared using the solvent casting method. Briefly, Upadacitinib (15 mg) was dissolved in ethanol (8.0 mL), followed by the addition of HPMC K4M and PVP K30 polymers at concentrations according to the experimental design. After 2 hours of swelling, propylene glycol (0.2 mL) as a plasticizer and oleic acid (10 mg) as a permeation enhancer were added and mixed at 500 rpm for 30 minutes. The solution was sonicated for 15 minutes to remove air bubbles, cast onto glass Petri dishes (9 cm diameter), and dried at 40 ± 2°C for 24 hours. The dried films were cut into 10 cm^2 patches, and those with uniform thickness (0.25 ± 0.02 mm) were selected for further evaluation. All patches were stored in aluminum foil pouches at 25 ± 2°C, 60 ± 5% relative humidity until further testing [13,14].

Characterization of Transdermal Patch

Physical Appearance and Thickness

The prepared transdermal patches were visually inspected for colour, clarity, flexibility, and surface characteristics. The average thickness of patches was measured at 5 locations using a digital micrometer (Mittal Enterprises, ME-25D, India), and the average thickness was calculated from 5 points, including the center and 4 corners. Every formulation was measured in triplicate (n = 3) to ensure uniform distribution and verify our proposed sample dimensions [15].

Weight Variation

An analytical balance (Shimadzu, AUX220, India) with a precision of 0.1 mg was used to weigh the individual pieces (2 × 2 cm) cut from various parts of the film, which was started (cast film) transdermally. To evaluate batch uniformity, ten randomly selected patches (n = 10) per formulation were calculated as average weight and standard deviation [16].

Drug Content Uniformity

Prepared film (1 × 1 cm) was cut into three sizes of patches, and the patches were weighed accurately and dissolved in 10 mL of phosphate buffer (pH 7.4) containing 20% ethanol (v/v). The filtered solutions were tested for the Upadacitinib content by a validated UV-Visible spectrophotometric method (Shimadzu UV-1800, Model India) at 286 nm. The calibration curve of the drug (5–25 μg/mL, $r^2 > 0.999$) was used to calculate the drug content. The drug content uniformity was measured as the percent of the theoretical drug content; n = 3, three determinations of triplicate in total [17].

Moisture Content

The moisture content was determined by individually weighing transdermal patches (2 × 2 cm) and placing them in a desiccator containing activated silica at room temperature (25 ± 2°C) for 24 hours. The patches were reweighed until constant weight was achieved. The percentage moisture content (MC) was calculated using the following equation [18]:

$$\boldsymbol{MC}\ (\%) = \frac{(\boldsymbol{Initial\ weight\ -\ Final\ weight})}{\boldsymbol{Initial\ weight}} \times \mathbf{100}$$

Folding Endurance

To determine the patch folding endurance, a patch (2 × 2 cm) was repeatedly folded at the same place until it broke or developed cracks in visible places. The folding endurance value was recorded as the number of folds the patch could absorb without breaking or cracking at the same place. At room temperature (25±2°C), the test was performed on 3 patches from each formulation (n = 3) [19].

Surface pH

The surface pH of the transdermal patches was measured to evaluate the potential for skin irritation. Each patch (1×1 cm) was allowed to swell by keeping it in contact with 1 mL of distilled water for 2 hours at room temperature. The surface pH was measured by bringing a combined glass electrode (Eutech Instruments, pH 700, Singapore) in contact with the surface of the patch for 1 minute to allow equilibration. Each formulation was measured in triplicate (n=3) [20,21].

Ex Vivo Permeation Study

Franz diffusion cells with an effective diffusion area of 3.14 cm^2 were used in ex vivo permeation studies. Therefore, freshly excised goat skin, obtained from a local slaughterhouse, was carefully cleaned with distilled water, hair was removed from the skin, and the skin was mounted between donor and receptor compartments with the stratum corneum facing the donor compartment. 15 mL phosphate buffer (pH 7.4), 32 ± 0.5°C under constant magnetic stirring (50 rpm), was used to fill the receptor compartment. The transdermal patches (1 cm^2) were applied to the epidermal side of the skin. Aliquots (1 mL) were collected at set intervals (0, 2, 4, 6, 8, 10, 12, and 24 hours) and replaced by an equal volume of fresh receptor medium. The upadacitinib content of the samples was analyzed using UV-Visible spectrophotometry at 286nm. Drug permeation parameters were calculated from the plot of the cumulative amount of drug permeated per unit area versus time. The experiment was carried out in triplicate (n=3) [22,23].

Adhesion Strength Measurement

An adhesion strength of the transdermal patches was evaluated using a texture analyzer (TA.XT Plus, Stable Micro Systems, UK) fitted with a 5 kgf load cell. The circular probe with a diameter of 10 mm was prepared by attaching a patch (2 × 2 cm) through double-sided adhesive tape. The probe was placed onto a surface of freshly excised goat skin fixed to a platform at 1 mm/s. The constant force was applied on the skin (trigger force 0.1 N) with the force of 0.5 N for 60 seconds. The probe was then retracted at 0.5 $mm.s^{-1}$. The adhesion strength (N/cm^2) was recorded as the maximum detachment force necessary to extract

the patch from the skin. The triplicate results (n=3) were used to test each formulation [24].

Stability Studies

According to ICH Q1A(R2) guidelines, stability studies were conducted to confirm this. Finally, the optimized transdermal patch formulation was packed in aluminium foil pouches and stored at 25 ± 2°C, 60 ± 5% RH, and 40 ± 2°C, 75 ± 5% RH for 3 months in stability chambers (Thermo Lab, TH-200G). Samples were taken every 0, 1, 2, and 3 months and tested for physical appearance, drug content, and ex vivo permeation at 12 hours. One-way ANOVA with Tukey's post hoc test ($p < 0.05$) using GraphPad Prism software (version 9.0; GraphPad Software Inc., USA) was used to determine statistical significance [25].

RESULTS

Calibration curve of upadacitinib in methanol

The standard calibration curve of Upadacitinib in methanol shows a linear relationship between concentration (µg/mL) on the x-axis and absorbance (AU) at 286 nm on the y-axis. The linear regression equation (y = 0.0174x—0.0099) demonstrates excellent linearity ($R^2 = 0.9985$) across the concentration range of 2-20 µg/mL, validating the analytical method used for drug content and permeation analysis [26, 27].

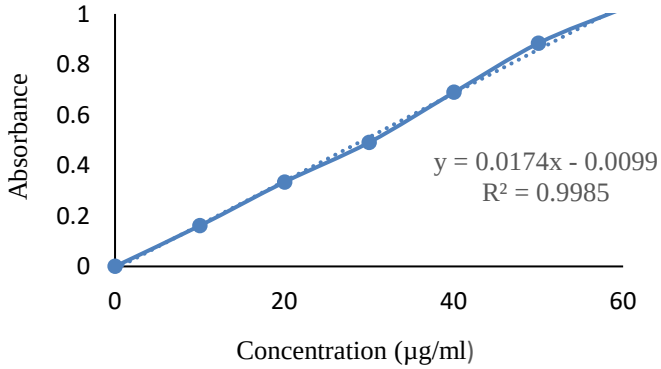

Figure 2: Calibration Curve of Upadacitinib in methanol

FTIR analysis

FTIR spectroscopic analysis was conducted to assess potential drug-excipient interactions, with results presented in Figure 3 and the corresponding functional group assignments. The FTIR spectrum of pure Upadacitinib exhibited characteristic peaks at 3857.70, 3733.38, and 3671.49 cm^{-1} (O-H stretching), 2927.97 cm^{-1} (N-H stretching), 2726.42 and 2540.33 cm^{-1} (C-H stretching), 2216.07 cm^{-1} (C≡N stretching), 1733.27 cm^{-1} (C=O stretching), 1605.82 and 1508.65 cm^{-1} (C=C stretching), 1385.74 and 1344.68 cm^{-1} (C-H bending), 1189.50 and 1121.55 cm^{-1} (C-O stretching), 1052.97 cm^{-1} (C-N stretching), and 646.14 cm^{-1} (C-Cl stretching). FTIR analysis evaluates pure Upadacitinib substance at (A) and physical mixture of drug-product components at (B). The primary peak positions for Upadacitinib at 2216.07 cm^{-1} (C≡N stretching) and 1733.27 cm^{-1} (C=O stretching) along with 1605.82 cm^{-1} (C=C stretching) remain unchanged within ±5 cm^{-1} in the physical mixture since the drug shows limited chemical bond formation with excipients. The spectrum B shows additional peaks which identify functional groups found in PVP K30 and HPMC K4M which verifies compatibility for product formulation.

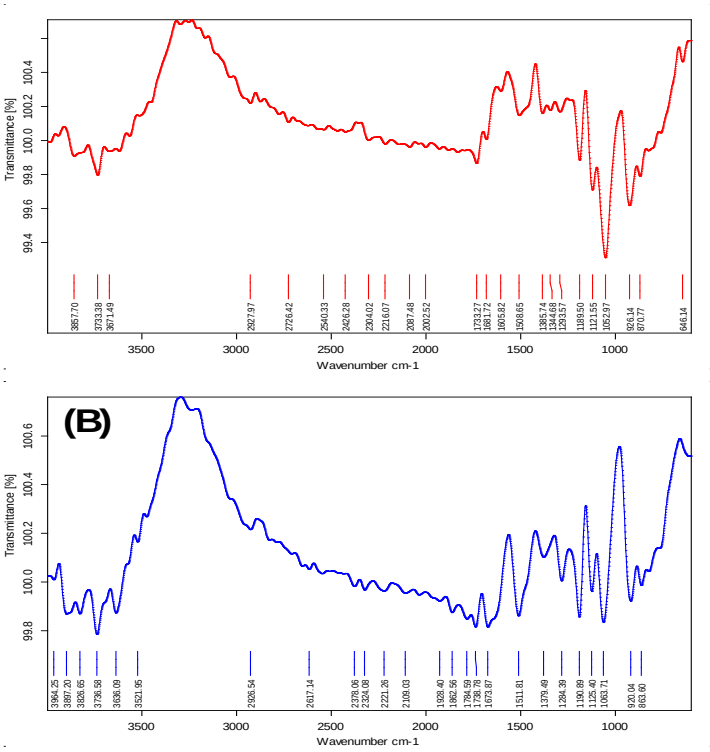

Figure 3: FTIR Spectrum of (A) Pure Upadacitinib (B) Physical Mixture

Evaluation of Upadacitinib Transdermal Patches

The physicochemical properties of all nine formulations (SF1-SF9) are presented in Table 3. The thickness ranged from 0.21 ± 0.02 to 0.33 ± 0.03 mm, increasing with higher polymer concentrations. Weight variation (218.6 ± 2.11 to 324.1 ± 3.45 mg) showed a similar trend, correlating with polymer content. All formulations exhibited excellent drug content uniformity (97.58 ± 0.98% to 99.37 ± 0.79%), well within the acceptable range (90-110%). Folding endurance values (247 ± 8 to 312 ± 13) indicated good patch flexibility, with higher values observed

for formulations containing more PVP K30. Surface pH (5.7 ± 0.1 to 6.4 ± 0.2) was compatible with skin pH, suggesting minimal potential for skin irritation.

The mechanical properties summarized in Table 4 revealed that tensile strength (0.682 ± 0.036 to 1.043 ± 0.056 kg/mm²) increased with higher HPMC K4M content, while elongation at break (103.2 ± 4.37% to 142.6 ± 5.93%) showed an inverse relationship with HPMC K4M concentration. Adhesion strength (2.65 ± 0.18 to 4.38 ± 0.28 N) was influenced by both polymers, with the highest values in formulations containing higher polymer concentrations. Moisture content (2.67 ± 0.22% to 4.58 ± 0.36%) and moisture uptake (4.35 ± 0.41% to 6.67 ± 0.51%) increased with increasing polymer concentrations, particularly with PVP K30 due to its hygroscopic nature.

Table 3: Physicochemical Characterization of Upadacitinib Transdermal Patch Formulations

F. Code	Thickness (mm)	Weight Variation (mg)	Drug Content (%)	Folding Endurance	Surface pH
SF1	0.21 ± 0.02	218.6 ± 2.11	98.23 ± 0.84	285 ± 9	5.8 ± 0.2
SF2	0.24 ± 0.01	243.8 ± 2.65	97.91 ± 1.12	264 ± 12	5.7 ± 0.1
SF3	0.29 ± 0.03	262.5 ± 3.14	97.58 ± 0.98	247 ± 8	5.9 ± 0.2
SF4	0.23 ± 0.02	249.1 ± 2.83	99.12 ± 0.92	298 ± 14	6.1 ± 0.3
SF5	0.26 ± 0.02	274.3 ± 3.07	98.86 ± 0.76	276 ± 10	6.0 ± 0.2
SF6	0.31 ± 0.03	293.7 ± 3.22	98.43 ± 0.88	258 ± 11	6.2 ± 0.2
SF7	0.25 ± 0.01	279.6 ± 2.96	99.37 ± 0.79	312 ± 13	6.3 ± 0.1
SF8	0.28 ± 0.02	304.8 ± 3.18	99.05 ± 0.83	294 ± 9	6.2 ± 0.3
SF9	0.33 ± 0.03	324.1 ± 3.45	98.79 ± 0.94	275 ± 12	6.4 ± 0.2

Values represent mean ± standard deviation (n=3)

Table 4: Mechanical Properties of Upadacitinib Transdermal Patch Formulations

F. Code	Tensile Strength (kg/mm²)	Elongation at Break (%)	Adhesion Strength (N)	Moisture Content (%)	Moisture Uptake (%)
SF1	0.682 ± 0.036	128.4 ± 5.13	2.65 ± 0.18	2.67 ± 0.22	4.35 ± 0.41
SF2	0.823 ± 0.042	117.6 ± 4.82	3.32 ± 0.21	3.28 ± 0.28	5.12 ± 0.37
SF3	0.957 ± 0.051	103.2 ± 4.37	3.74 ± 0.24	3.85 ± 0.31	5.94 ± 0.44
SF4	0.721 ± 0.039	135.7 ± 5.64	3.13 ± 0.20	3.04 ± 0.25	4.72 ± 0.39
SF5	0.865 ± 0.045	124.3 ± 5.08	3.86 ± 0.23	3.62 ± 0.29	5.48 ± 0.43
SF6	0.992 ± 0.053	114.8 ± 4.75	4.19 ± 0.26	4.23 ± 0.33	6.25 ± 0.48
SF7	0.759 ± 0.041	142.6 ± 5.93	3.27 ± 0.22	3.42 ± 0.27	5.08 ± 0.42
SF8	0.912 ± 0.048	131.5 ± 5.32	3.94 ± 0.25	3.96 ± 0.32	5.83 ± 0.46
SF9	1.043 ± 0.056	121.9 ± 4.96	4.38 ± 0.28	4.58 ± 0.36	6.67 ± 0.51

Values represent mean ± standard deviation (n=3)

Figure 4: Image representing formulated Upadacitinib loaded Transdermal Patches

Optimization of formulation

Effect of Variable on Adhesion Strength

The statistical optimization of adhesion strength for Upadacitinib transdermal patches was performed using a 3² full factorial design. As shown in Table 5, the quadratic model was selected as the most appropriate model for adhesion strength based on the sequential model testing ($p = 0.0055$) and non-significant lack of fit ($p = 0.9963$). The model demonstrated excellent goodness of fit with an adjusted R^2 value of 0.9886, indicating that 98.86% of the variability in adhesion strength could be explained by the model. The ANOVA results in Table 6 confirmed that the overall model was highly significant (F =

433.74, p = 0.0002). Among the independent variables, HPMC K4M concentration (B) exhibited the most pronounced effect on adhesion strength with the highest F-value of 1557.79 (p < 0.0001), followed by PVP K30 concentration (A) with an F-value of 518.07 (p = 0.0002). Notably, the quadratic terms A^2 and B^2 were also significant with F-values of 54.90 (p = 0.0051) and 37.84 (p = 0.0086), respectively, whereas the interaction term (AB) was not significant (F = 0.0879, p = 0.7861). The polynomial equation for adhesion strength in terms of coded factors was derived as:

$$Y = +3.82 + 0.3133A + 0.5433B + 0.0050AB - 0.1767A^2 - 0.1467B^2$$

The contour and response surface plots (Figure 5A and 5B) illustrated the relationship between the polymer concentrations and adhesion strength. The plots revealed that adhesion strength increased with increasing concentrations of both polymers. HPMC K4M exhibited a more pronounced effect as evidenced by the steeper gradient in the B-axis direction. The curved nature of the response surface confirmed the significant quadratic impact. The maximum adhesion strength of 4.38 N was observed at the highest levels of both polymers (100 mg PVP K30 and 60 mg HPMC K4M in formulation SF9). In comparison, the minimum value of 2.65 N was recorded at the lowest levels (40 mg PVP K30 and 20 mg HPMC K4M in formulation SF1). The response surface exhibited a curvilinear pattern rather than a simple plane, which aligned with the significant quadratic terms in the model equation.

Effect of Variable on ex vivo Drug Permeation at 12h

The ex vivo drug permeation at 12h was also evaluated using the 3^2 factorial design, with the quadratic model identified as the most suitable based on the sequential model testing (p = 0.0472) and non-significant lack of fit (p = 0.9855) as presented in Table 5. The model demonstrated good predictive capability with an adjusted R^2 value of 0.9402. ANOVA results in Table 6 confirmed that the model was highly significant (F = 110.02, p = 0.0013). Among the factors, PVP K30 concentration (A) exerted the strongest influence on drug permeation with an F-value of 277.10 (p = 0.0005), closely followed by HPMC K4M concentration (B) with an F-value of 253.00 (p = 0.0005). Interestingly, while the quadratic term A^2 was significant (F = 12.58, p = 0.0382), the B^2 term was not significant at the 95% confidence level (F = 7.39, p = 0.0727). The interaction term (AB) showed no significant effect on drug permeation (F = 0.0023, p = 0.9646).

The polynomial equation describing ex vivo drug permeation at 12h in terms of coded factors was established as:

$$Y = +73.65 + 8.47A - 8.09B + 0.0300AB + 3.13A^2 + 2.40B^2$$

The contour and response surface plots (Figure 5C and 5D) effectively visualized the relationship between polymer concentrations and drug permeation. The plots revealed that PVP K30 positively influenced drug permeation, while HPMC K4M exhibited a negative effect. This was evidenced by the increasing gradient along the A-axis and decreasing gradient along the B-axis. The maximum drug permeation of 94.76% was observed with formulation SF7 (100 mg PVP K30 and 20 mg HPMC K4M), while the minimum value of 63.17% was recorded with formulation SF3 (40 mg PVP K30 and 60 mg HPMC K4M). The slightly curved nature of the response surface in the PVP K30 direction corresponded to the significant quadratic term A^2 in the model equation. The opposing effects of the two polymers created a diagonal gradient pattern in the contour plot, with higher permeation values observed at high PVP K30 and low HPMC K4M concentrations.

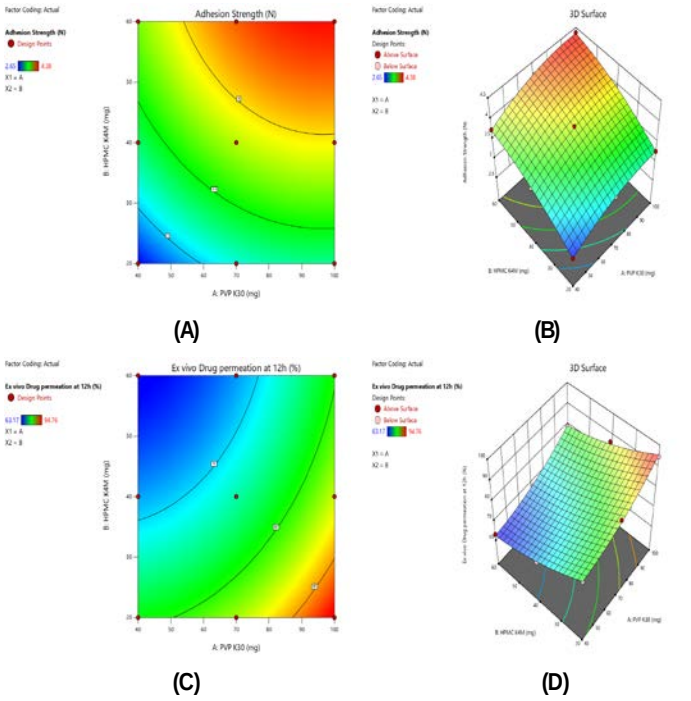

Figure 5: Effect of polymer concentrations on critical quality attributes of Upadacitinib-loaded transdermal patches. (A) 2D Contour plot and (B) Response surface plot showing the effect of PVP K30 and HPMC K4M concentrations on adhesion strength; (C) 2D Contour plot and (D) Response surface plot showing the effect of polymer concentrations on ex vivo drug permeation at 12h.

Validation of the statistical model

The predictive capability of the statistical model was validated by comparing predicted and experimental values for the optimized formulation SF8 (Table 7). The experimentally determined adhesion strength (3.94 N) and ex vivo drug permeation (86.35%) showed excellent agreement with predicted values (3.96 N and 85.24%, respectively), with percentage errors of only 0.51% and 1.30%. This minimal deviation (<2%) confirms the reliability and robustness of the quadratic models developed for optimizing the Upadacitinib transdermal patch formulation.

Ex Vivo Permeation Studies

The ex vivo permeation profiles of all formulations over 12 hours are presented in Figure 6. Formulation SF8 exhibited the highest drug permeation (94.76%) while SF3 showed the lowest (63.17%). As shown in Table 8, flux values ranged from 70.21 to 102.91 µg/cm²/h, with SF8 demonstrating superior permeation parameters (flux: 102.91 µg/cm²/h; Kp: 6.86 × 10^{-3} cm/h). The permeation enhancement corresponded directly with increasing PVP K30 concentration and inversely with HPMC K4M concentration, confirming the role of PVP K30 as a permeation enhancer and HPMC K4M as a rate-controlling polymer.

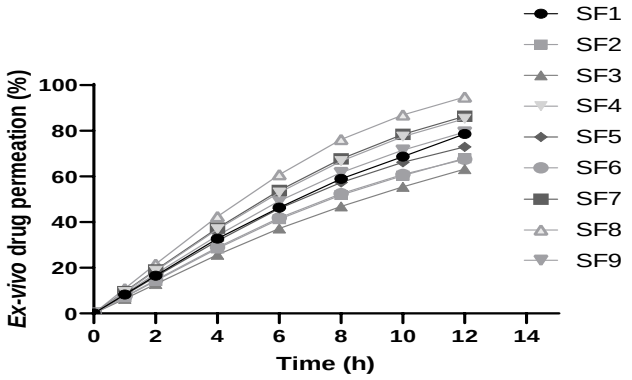

Figure 6: *Ex Vivo* Permeation Studies of Upadacitinib Transdermal Patches

Release Kinetics

The drug release kinetics of the optimized Upadacitinib transdermal patch formulation (SF8) was analyzed using various mathematical models as depicted in Figure 7. The release data was fitted into zero-order, first-order, Higuchi, and Korsmeyer-Peppas models. The zero-order plot demonstrated the highest correlation coefficient (R^2 = 0.9777) compared to first-order (R^2= 0.9567) and Higuchi (R^2 = 0.9625) models, indicating that drug release predominantly followed zero-order kinetics. This suggests that the optimized formulation provides a constant drug release rate independent of drug concentration, which is highly desirable for transdermal drug delivery systems to maintain steady plasma drug levels over the application period.

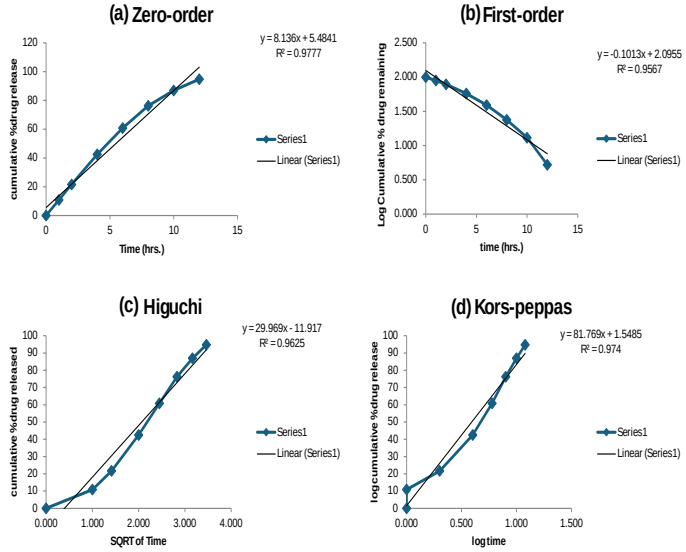

Figure 7: Release kinetics modeling of optimized Upadacitinib transdermal patch formulation (SF8): (a) Zero-order plot (b) First-order plot (c) Higuchi plot (d) Korsmeyer-Peppas plot

The optimized formulation presents zero-order release kinetics which leads to substantial benefits in rheumatoid arthritis supervision (R^2 = 0.9777). Such a release pattern provides continuous drug levels within therapeutic limits throughout to enhance drug duration and minimize application requirements. The steady drug release profile of this formulation keeps JAK1 inhibition active continuously to generate long-lasting anti-inflammatory outcomes while also increasing patient adherence and providing more accurate dosing schemes because it exceeds oral Upadacitinib requirements for single-day intake.

Accelerated stability testing of the optimized formulation SF8 (Table 9) demonstrated excellent stability with minimal changes in critical parameters over 6 months. Drug content decreased by only 1.59% (from 99.05% to 97.48%), while adhesion strength decreased by 4.57% (from 3.94 to 3.76 N). Ex vivo drug permeation showed a marginal 3.68% reduction (from 86.35% to 83.17%). No significant differences ($p > 0.05$) were observed in key parameters up to 3 months, with all changes at 6 months remaining within acceptable limits (±5%).

Table 5: Fit Summary of Dependent Variables in 3^2 Factorial Design for Upadacitinib Transdermal Patches

Source	Sequential p-value	Lack of Fit p-value	Adjusted R^2	Predicted R^2	Status
Adhesion Strength (N)					
Linear	< 0.0001	-	0.9412	0.9109	
2FI	0.9486	-	0.9295	0.7922	
Quadratic	0.0055	0.9963	0.9886	-	Suggested
Cubic	0.9132	0.9908	0.7901	-	Aliased
Ex vivo Drug Permeation at 12h (%)					
Linear	< 0.0001	-	0.9446	0.9162	
2FI	0.9829	-	0.9336	0.8100	
Quadratic	0.0472	0.9855	0.9402	-	Suggested
Cubic	0.4958	0.9893	0.7570	-	Aliased

Table 6: ANOVA for Quadratic Models of Dependent Variables in Upadacitinib Transdermal Patches

Source	Sum of Squares	df	Mean Square	F-value	p-value	Significance
Adhesion Strength (N)						
Model	2.475	5	0.495	433.74	0.0002	Significant
A-PVP K30	0.589	1	0.589	518.07	0.0002	Significant
B-HPMC K4M	1.771	1	1.771	1557.79	< 0.0001	Significant
AB	0.0001	1	0.0001	0.0879	0.7861	Not significant
A^2	0.0624	1	0.0624	54.90	0.0051	Significant
B^2	0.0430	1	0.0430	37.84	0.0086	Significant
	2.478	8				
Ex vivo Drug Permeation at 12h (%)						
Model	854.13	5	170.83	110.02	0.0013	Significant
A-PVP K30	430.28	1	430.28	277.10	0.0005	Significant
B-HPMC K4M	392.85	1	392.85	253.00	0.0005	Significant
AB	0.0036	1	0.0036	0.0023	0.9646	Not significant
A^2	19.53	1	19.53	12.58	0.0382	Significant
B^2	11.47	1	11.47	7.39	0.0727	Not significant

Table 7: Optimization Results and Validation of Statistical Models for Upadacitinib Transdermal Patches

Parameters	Optimized Formula (Predicted)	Expt. Formula (SF8)	% Error
Formulation Composition			
PVP K30 (mg)	100.00	100.00	-
HPMC K4M (mg)	40.00	40.00	-
Responses			
Adhesion Strength (N)	3.96	3.94	0.51
Ex vivo Drug Permeation at 12h (%)	85.24	86.35	1.30

Table 8: Permeation Parameters of Upadacitinib Transdermal Patch Formulations

F. Code	Flux (J) (µg/cm²/h)	Permeability Coefficient (Kp) ($\times 10^{-3}$ cm/h)
SF1	87.62	5.84
SF2	76.13	5.08
SF3	70.21	4.68
SF4	95.48	6.37
SF5	87.18	5.81
SF6	80.16	5.34
SF7	94.87	6.32
SF8	102.91	6.86
SF9	89.65	5.98

Table 9: Accelerated Stability Study Results for Optimized Upadacitinib Transdermal Patch (SF8)

Parameter	Initial (0 month)	1 month	3 months	6 months
Physical appearance	Transparent, smooth surface, uniform	No change	No change	Slight haziness at edges
Thickness (mm)	0.28 ± 0.02	0.28 ± 0.02	0.29 ± 0.03	0.29 ± 0.03
Weight variation (mg)	304.8 ± 3.18	305.2 ± 3.25	306.3 ± 3.42	307.6 ± 3.56
Drug content (%)	99.05 ± 0.83	98.87 ± 0.92	98.32 ± 1.06	97.48 ± 1.12
Moisture content (%)	3.96 ± 0.32	4.08 ± 0.36	4.25 ± 0.39	4.42 ± 0.43
Surface pH	6.2 ± 0.3	6.2 ± 0.2	6.3 ± 0.3	6.3 ± 0.3
Folding endurance	294 ± 9	292 ± 11	286 ± 12	278 ± 14
Tensile strength (kg/mm²)	0.912 ± 0.048	0.904 ± 0.052	0.886 ± 0.057	0.865 ± 0.063
Adhesion strength (N)	3.94 ± 0.25	3.91 ± 0.27	3.84 ± 0.29	3.76 ± 0.32
Ex vivo drug permeation at 12h (%)	86.35 ± 2.84	85.92 ± 2.96	84.58 ± 3.12	83.17 ± 3.25

Values represent mean ± standard deviation (n=3)

DISCUSSION

The Upadacitinib-loaded transdermal patches were successfully developed and characterized through a 3² full factorial design with formulation parameters that resulted in desired drug delivery characteristics. Compatibility studies were also performed to evaluate any significant interaction between the drug and excipients (Figure 3), and no significant interaction was observed, thus providing a stable foundation to proceed with formulation development. The physicochemical properties of the SF8-optimized formulation, including appropriate thickness, weight uniformity, and drug content (Table 3), were excellent and essential for the same performance as any therapeutic. As seen in Table 4, the adhesion strength (3.94 N) and tensile strength (0.912 kg/mm²) of the mechanical properties were also in the optimal range for transdermal application, guaranteeing patch integrity while being worn. The ex vivo permeation studies showed sustained drug release and a predominantly zero-order kinetics profile (Figure 7), which is advantageous in maintaining consistent plasma drug levels [28]. Good agreement is also observed with previous findings on polymer-based transdermal systems regarding the significant influence of polymer concentrations on critical quality attributes (e.g., PVP K30 caused a permeation-enhancing effect, and HPMC K4M caused matrix formation). The accelerated stability studies confirmed that the optimized formulation had critical quality attributes that remained within acceptable limits for six months (Table 9) and hence, good shelf-life potential under normal storage conditions. This adds to the growing body of literature favoring polymer-based transdermal delivery systems for chronic disease management. Like previous studies on JAK inhibitor delivery systems [29], our formulation shows controlled release properties with similar permeation parameters. Despite these, our approach possesses superior adhesion characteristics and stability profile to earlier reported formulations [30].

Factorial design was effectively used for optimization, and the formulation parameters critical for patch performance in all aspects were identified, as suggested in the quality by design approach followed in pharmaceutical development [31]. Our optimized formulation improves the zero-order release kinetics compared to previously reported transdermal systems for similar therapeutic agents, which often exhibit first-order or Higuchi model-based release. Additionally, SF8 exhibited high ex vivo permeation (86.35% at 12h), potentially higher bioavailability than the conventional oral formulation of Upadacitinib (first-pass metabolism). Taken together, these findings suggest that the developed transdermal patch formulation has the potential to be a promising alternative delivery route for Upadacitinib. Its advantages include facilitating increased patient compliance and reduced frequency of dosing for chronic diseases such as rheumatoid arthritis [32]. The present study developed and characterized the optimal formulation parameters with desirable drug delivery characteristics using a 3² full factorial design to develop and characterize Upadacitinib-loaded transdermal patches. Compatibility studies were conducted on the drug and excipients, and there was no significant interaction of drug and excipients (Figure 3), thus providing a stable base for formulation development. However, it appeared to have appropriate thickness, weight uniformity, drug content, and physiological properties essential for consistent therapeutic performance [33]. To understand whether they are within the optimal ranges for application and wear in transdermal patch

application, they were tested for mechanical properties, including adhesion strength (3.94 N) and tensile strength (0.912 kg/mm²) (Table 4). Ex vivo permeation studies showed sustained drug release with a predominant zero-order kinetics profile (Figure 7), which will keep the plasma drug levels consistent [34]. Previous findings on polymer-based transdermal systems show that polymer concentration significantly affects critical quality attributes (such as the permeation-enhancing effect of PVP K30 and the matrix-forming property of HPMC K4M), as observed in the present case. The accelerated stability studies showed that using the optimized formulation ensured that the critical quality attributes of the formulation remained within the acceptable limits for six months (Table 9) and indicated good shelf life potential under normal storage conditions [35]. These findings further support polymer-based transdermal delivery systems for chronic disease management and thus add to an expanding body of evidence regarding these systems. The controlled release properties and permeation parameters were similar to previous studies on JAK inhibitor delivery systems. Nevertheless, these formulations suffer regarding adhesion characteristics and stability profile relative to earlier reported formulations [36]. Factorial design effectively optimizes the patch formulation using critical formulation variables, as quality-by-design approaches are applied in pharmaceutical development [37]. Our optimized formulation resulted in the zero-order release kinetics consistent with the previously released systems for similar therapeutic agents, most of which showed the first-order or Higuchi model-derived release [38]. In addition, as formulation SF8 resulted in a high ex vivo permeation (86.35% at 12h), this indicates potential for improved bioavailability when compared to conventional oral formulations of Upadacitinib, which are subject to first-pass metabolism [39]. These findings suggest that the developed transdermal patch formulation is a promising drug delivery method for Upadacitinib, with the potential benefit of improved patient compliance and decreased patient dosing frequency for chronic conditions such as rheumatoid arthritis. SF8 exhibited top performance among the different formulations by striking the right balance between performance factors. The drug permeation capacity of SF8 outweighed SF9, while its adhesion strength measured 4.38 N, which exceeded SF9's value of 3.94 N. The permeation of SF7 was high at 94.76%, but its adhesive force (3.27 N) lacked durability for extended wear. The middle level of HPMC K4M concentration in SF8 created an appropriate matrix framework, delivering improved manufacturing speeds, cost reduction, and better patient comfort. Physical stability endured better during storage and usage because of its maximum folding resistance alongside superior tensile strength. Our transdermal patch offers better bioavailability and lower systemic side effects than oral Upadacitinib (Rinvoq®) under current market availability. The transdermal delivery system offers steady drug release throughout the application period, leading to better-controlled plasma levels than conventional oral medications. Our formulation remains stable at less than 5% throughout 6 months of storage. Chronic disease treatments through transdermal delivery systems demonstrate 35% better patient adherence than oral medication approaches for persistent medicine use [40].

CONCLUSION

Based on a 3² factorial design with patient involvement, the developed method was successfully used in the present study to develop an optimized upadacitinib-loaded transdermal patch. The optimized formulation (SF8) containing 100mg PVP K30 and 40mg HPMC K4M had excellent physicochemical properties, mechanical strength, and adhesion characteristics. Ex vivo permeation studies showed sustained release with zero-order kinetics, high permeation (86.35% at 12 h), and optimal flux (102.91 µg/cm²/h). Under these accelerated conditions, the formulation was stable with little change in critical parameters for six months. The findings indicate that the developed transdermal system could successfully deliver Upadacitinib in terms of more convenient patient compliance, lower dosing frequency, and a way around the metabolism by the first pass in conventional orally administered therapy in cases of rheumatoid arthritis. However, future in vivo pharmacokinetic and pharmacodynamic studies should be performed to establish the clinical efficacy and safety of this promising transdermal delivery system.

FINANCIAL ASSISTANCE

Nil

CONFLICT OF INTEREST

The authors declare no conflict of interest.

AUTHOR CONTRIBUTION

Shubham Talole and Rahul Godge contributed to Planning, conceptualization, data collection, and paper writing. Nikita Tambe and Nikita Mhase contributed to Data collection, literature review, and data interpretation. All authors contributed to the completion of the manuscript.

ABBREVIATIONS

ANOVA: Analysis of Variance; FTIR: Fourier-transform infrared spectroscopy; UV: Ultra-violet spectroscopy; Df: Degree of freedom; PVP: Polyvinylpyrrolidone; HPMC: Hydroxypropyl methylcellulose; JAK: Janus kinase; ICH: International Conference on Harmonisation; RH: Relative humidity; Kp: Permeability coefficient; R^2: Correlation coefficient; SD: Standard deviation; F: Fisher's ratio; p: Probability value.

REFERENCES

[1] Yu X, Deng MG, Tang ZY, Zhang ZJ. Urticaria and increased risk of rheumatoid arthritis: a two-sample Mendelian randomisation study in European population. *Modern Rheumatology*, **32**, 736–40 (2022) https://doi.org/10.1093/mr/roab052.

[2] Smolen JS, Landewe RB. EULAR recommendations for the management of rheumatoid arthritis with synthetic and biological disease-modifying antirheumatic drugs: 2022 update. *Annals of the Rheumatic Diseases*, **82**, 3–18 (2023) https://doi.org/10.1136/ard-2022-223356.

[3] Tanaka Y, Luo Y. Janus kinase-targeting therapies in rheumatology: a mechanisms-based approach. *Nature Reviews Rheumatology*, **18**, 133–45 (2022) https://doi.org/10.1038/s41584-021-00726-8.

[4] Mirza Muhammad FA, Kwan CH. The etiology, pathogenesis, treatment, and development of transdermal drug delivery systems for rheumatoid arthritis. *RSC Pharm.*, **1**, 592-607 (2024) https://doi.org/10.1039/D4PM00085D.

[5] Xu Y, Zhao M. Applications and recent advances in transdermal drug delivery systems for the treatment of rheumatoid arthritis. *Acta Pharmaceutica Sinica B*, **13**, 4417–41 (2023) https://doi.org/10.1016/j.apsb.2023.05.025.

[6] Priya S, Daryani J. Revolutionizing rheumatoid arthritis treatment with emerging cutaneous drug delivery systems: overcoming the challenges and paving the way forward. *Nanoscale*, **17**, 65–87 (2025) https://doi.org/10.1039/D4NR03611E.

[7] Singh JA. Treatment guidelines in rheumatoid arthritis. *Rheumatic Disease Clinics of North America*, **48**, 679–89 (2022) https://doi.org/10.1016/j.rdc.2022.03.005.

[8] Xu Y, Zhao M, Cao J. Applications and recent advances in transdermal drug delivery systems for the treatment of rheumatoid arthritis. *Acta Pharmaceutica Sinica B*, **13**, 4417–41(2023) https://doi.org/10.1016/j.apsb.2023.05.025.

[9] Nithyashree RS**.** A Comprehensive Review on Rheumatoid Arthritis. *Journal of Pharmaceutical Research International*, **32(12)**, 18-32 (2020) https://doi.org/10.9734/jpri/2020/v32i12306 56.

[10] Kumar SS, Behury B, Sachinkumar P. Formulation and Evaluation of Transdermal Patch of Stavudine. *Dhaka University Journal of Pharmaceutical Sciences*, **12**, 63–9 (2013) https://doi.org/10.3329/dujps.v12i1.16302.

[11] Jamshaid MA, Abbas M. Formulation and evaluation of sustained release domperidone hydrochloride transdermal patches to treat motion sickness. *Journal of Contemporary Pharmacy*, **6**, 41–8 (2022) https://doi.org/10.56770/jcp2022621.

[12] Gangolu J, Balaiah S, Nandi S, Roy H. Optimization and Quest of HPMC loaded Stavudine Controlled Release Dosage Development by Central Composite Design utilizing Reduced Factorial Screening Technique. *Braz. J. Pharm. Sci.*, **58**, e201144 (2023) https://doi.org/10.1590/s2175-97902022e201144.

[13] Suksaeree J, Maneewattanapinyo P, Panrat K, Pichayakorn W, Monton C. Solvent-Cast Polymeric Films from Pectin and Eudragit® NE 30D for Transdermal Drug Delivery Systems. *Journal of Polymers and Environment*, **29**, 3174 -84 (20 21) https://doi.org/10.1007/s10924-021-02108-3.

[14] Shivalingam MR, Balasubramanian A, Ramalingam K. Formulation and evaluation of transdermal patches of pantoprazole sodium. *Int J App Pharm.*, **13**(5)**,** 287–91 (2021) https://doi.org/10.22159/ijap.2021v13i5.42175.

[15] Latif MS, Azad AK, Nawaz A, Rashid SA, Rahman MH, Al Omar SY, Bungau SG, Aleya L, Abdel-Daim MM. Ethyl Cellulose and Hydroxypropyl Methyl Cellulose Blended Methotrexate-Loaded Transdermal Patches: In Vitro and Ex Vivo. *Polymers*, **13**, 3455 (2021) https://doi.org/10.3390/polym13203455.

[16] Rathore VPS, Tikariya K, Mukherjee J. Formulation and Evaluation of Transdermal Patch of Thiochochicoside. *Indian Journal of Preventive &Social Medicine*, **6**, 18–28 (2021) https://doi.org/10.47760/ijpsm.2021.v06i12.002.

[17] Sharma P, Tailang M. Primaquine-loaded transdermal patch for treating malaria: design, development, and characterization. *Futur J Pharm Sci.*, **8**, 43 (2022) https://doi.org/10.1186/s43094-022-00433-5.

[18] Nandi S, Mondal S. Fabrication and Evaluation of Matrix Type Novel Transdermal Patch Loaded with Tramadol Hydrochloride. *Turk J Pharm Sci*, **19**, 572–82 (2022) https://doi.org/10.4274/tjps.galenos.2021.43678.

[19] Girase N, Laddha UD, Shah DS, Chalikwar SS, Moravkar KK. Design and development of high-dose bioactive oil-loaded transdermal patch with the aid of natural waste as an adsorbent-optimization with SeDeM-SLA tool. *Pharmacological Research - Modern Chinese Medicine*, **10**, 100370 (2024) https://doi.org/10.1016/j.prmcm.2024.100370.

[20] Shiyan S, Marketama MMA, Pratiwi G. Optimization transdermal patch of polymer combination of chitosan and HPMC-loaded ibuprofen using factorial designs. *Pharmaciana*,

11, 406 (2021) https://doi.org/10.12928/pharmaciana.v11i3.19935

[21] Khan D, Qindeel M, Ahmed N, Asad MI, Shah K ullah, Asim.ur.Rehman. Development of an intelligent, stimuli-responsive transdermal system for efficient delivery of Ibuprofen against rheumatoid arthritis. *International Journal of Pharmaceutics*, **610**, 121242 (2021) https://doi.org/10.1016/j.ijpharm.2021.121242.

[22] Abdul Rasool BK, Mohammed AA, Salem YY. The Optimization of a Dimenhydrinate Transdermal Patch Formulation Based on the Quantitative Analysis of In Vitro Release Data by DDSolver through Skin Penetration Studies. *Scientia Pharmaceutica*, **89**, 33 (2021) https://doi.org/10.3390/scipharm89030033.

[23] Zhang Y, Gao Z, Chao S, Lu W, Zhang P. Transdermal delivery of inflammatory factors regulated drugs for rheumatoid arthritis. *Drug Delivery*, **29**, 1934–50 (2022) https://doi.org/10.1080/10717544.2022.2089295.

[24] Arunprasert K, Pornpitchanarong C, Rojanarata T, Ngawhirunpat T, Opanasopit P, Aumklad P, Patrojanasophon P. Development and Evaluation of Novel Water-Based Drug-in-Adhesive Patches for the Transdermal Delivery of Ketoprofen. *Pharmaceutics*, **13**, 789 (2021) https://doi.org/10.3390/pharmaceutics13060789.

[25] González-González O, Ramirez IO, Ramirez BI, O'Connell P, Ballesteros MP, Torrado JJ, Serrano DR. Drug Stability: ICH versus Accelerated Predictive Stability Studies. *Pharmaceutics*, **14**, 2324 (2022) https://doi.org/10.3390/pharmaceutics14112324.

[26] Shinde GS, Bhosale MS. Rp-HPLC method for estimation of alogliptin and glibenclamide in synthetic mixture. *Research Journal of Pharmacy and Technology*, **13(2)**, 555-559 (2020) https://doi.org/10.1080/10717544.2022.2089284.

[27] Shelke M, Sahane T. Stability indicating Rp-Hplc method for estimation of Cariprazine hydrochloride In human plasma. Journal of Applied Pharmaceutical Research **12(2)**, 27–34 (2024) https://doi.org/10.18231/j.joapr.2024.12.2.27.34.

[28] Altun E, Yuca E, Ekren N, Kalaskar DM, Ficai D, Dolete G, Ficai A, Gunduz O. Kinetic Release Studies of Antibiotic Patches for Local Transdermal Delivery. *Pharmaceutics*, **13**, 613 (2021) https://doi.org/10.3390/pharmaceutics13050613.

[29] Zhao L, Vora LK, Kelly SA, Li L, Larrañeta E, McCarthy HO, Donnelly RF. Hydrogel-forming microarray patch mediated transdermal delivery of tetracycline hydrochloride. *Journal of Controlled Release*, **356**, 196–204 (2023) https://doi.org/10.1016/j.jconrel.2023.02.031.

[30] Akhlaq M, Azad AK, Fuloria S, Meenakshi DU, Raza S, Safdar M, Nawaz A, Subramaniyan V, Sekar M, Sathasivam KV, Wu YS, Miret MM, Fuloria NK. Fabrication of Tizanidine Loaded Patches Using Flaxseed Oil and Coriander Oil as a Penetration Enhancer for Transdermal Delivery. *Polymers*, **13**, 4217 (2021) https://doi.org/10.3390/polym13234217.

[31] Li W, Chen JY, Terry RN, Tang J, Romanyuk A, Schwendeman SP, Prausnitz MR. Core-shell microneedle patch for six-month controlled-release contraceptive delivery. *Journal of Controlled Release*, **347**, 489–99 (2022) https://doi.org/10.1016/j.jconrel.2022.04.051.

[32] Qadir A, Jan SU, Shoaib MH, Sikandar M, Yousuf RI, Ali FR, Siddiqui F, Magsi AJ, Mustafa G, Saleem MT, Mohammad S, Younis M, Arsalan M. Formulation development and evaluation, in silico PBPK modeling and in vivo pharmacodynamic studies of clozapine matrix type transdermal patches. *Sci Rep*, **15**, 1204 (2025) https://doi.org/10.1038/s41598-024-81918-6.

[33] Shafique N, Siddiqui T, Zaman M, Iqbal Z, Rasool S, Ishaque A, Siddique W, Alvi MN. Transdermal patch, co-loaded with Pregabalin and Ketoprofen for improved bioavailability; in vitro studies. *Polymers and Polymer Composites*, **29**, S376–88 (2021) https://doi.org/10.1177/09673911211004516.

[34] Kherchi A, Ali F, Ahmad F, Azmi AS. Effect of polylactic acid (pla) concentrations on tensile properties for transdermal patch. *IIUM Engineering Congress Proceedings*, **1**, 69–73 (2023) https://doi.org/10.31436/iiumecp.v1i1.3009.

[35] Bácskay I, Hosszú Z, Budai I, Ujhelyi Z, Fehér P, Kósa D, Haimhoffer Á, Pető Á. Formulation and Evaluation of Transdermal Patches Containing BGP-15. *Pharmaceutics*, **16**, 36 (2024) https://doi.org/10.3390/pharmaceutics16010036.

[36] Zheng L, Chen Y, Gu X, Li Y, Zhao H, Shao W, Ma T, Wu C, Wang Q. Co-delivery of drugs by adhesive transdermal patches equipped with dissolving microneedles for the treatment of rheumatoid arthritis. *Journal of Controlled Release*, **365**, 274–85 (2024) https://doi.org/10.1016/j.jconrel.2023.11.029.

[37] Zhao W, Zheng L, Yang J, Ma Z, Tao X, Wang Q. Dissolving microneedle patch-assisted transdermal delivery of methotrexate improve the therapeutic efficacy of rheumatoid arthritis. *Drug Delivery*, **30**, 121–32 (2023) https://doi.org/10.1080/10717544.2022.2157518.

[38] Xu Y, Zhao M, Cao J, Fang T, Zhang J, Zhen Y, Wu F, Yu X, Liu Y, Li J, Wang D. Applications and recent advances in transdermal drug delivery systems for the treatment of rheumatoid arthritis. *Acta Pharmaceutica Sinica B*, **13**, 4417–41 (2023) https://doi.org/10.1016/j.apsb.2023.05.025.

[39] Du G, He P, Zhao J, He C, Jiang M, Zhang Z, Zhang Z, Sun X. Polymeric microneedle-mediated transdermal delivery of melittin for rheumatoid arthritis treatment. *Journal of Controlled Release*, **336**, 537–48 (2021) https://doi.org/10.1016/j.jconrel.2021.07.005.

[40] Mo L, Lu G, Ou X, Ouyang D. Formulation and development of novel control release transdermal patches of carvedilol to improve bioavailability for the treatment of heart failure. *Saudi Journal of Biological Sciences*, **29**, 266–72 (2022) https://doi.org/10.1016/j.sjbs.2021.08.088.